Controlling Hamiltonian chaos

Ying-Cheng Lai
Laboratory for Plasma Research, University of Maryland, College Park, Maryland 20742
and Department of Biomedical Engineering, The Johns Hopkins University School of Medicine, Baltimore, Maryland 21205

Mingzhou Ding
Center for Complex Systems, Florida Atlantic University, Boca Raton, Florida 33431
and Department of Mathematics, Florida Atlantic University, Boca Raton, Florida 33431

Celso Grebogi
Laboratory for Plasma Research, University of Maryland, College Park, Maryland 20742;
Institute for Physical Science and Technology, University of Maryland, College Park, Maryland 20742;
and Department of Mathematics, University of Maryland, College Park, Maryland 20742
(Received 2 September 1992)

The method for stabilizing an unstable periodic orbit in chaotic dynamical systems originally formulated by Ott, Grebogi, and Yorke (OGY) is not directly applicable to chaotic Hamiltonian systems. The reason is that an unstable periodic orbit in such systems often exhibits complex-conjugate eigenvalues at one or more of its orbit points. In this paper we extend the OGY stabilization method to control Hamiltonian chaos by incorporating the notion of stable and unstable directions at each periodic point. We also present an algorithm to calculate the stable and unstable directions. Other issues specific to the control of Hamiltonian chaos are also discussed.

PACS number(s): 05.45.+b

I. INTRODUCTION

In a recent paper, Ott, Grebogi, and Yorke (OGY) proposed a method to control chaos in nonlinear dynamical systems [1]. Their idea is based on the observation that a chaotic attractor has embedded within it an infinite number of unstable periodic orbits. By applying small, judiciously chosen temporal perburtations to an accessible parameter of the system, they demonstrated that an originally chaotic trajectory can be converted to a desired periodic orbit. A major advantage of the method is that it does not require *a priori* knowledge of the system equations. A time series from measuring one of the system's dynamical variables is generally sufficient to achieve the desired control [1–3]. Another advantage of the method lies in one's flexibility to choose and control, in principle, any one of the unstable periodic orbits in the attractor. One chooses the one that gives the best system performance according to some criterion. This method has since attracted growing interest and it has been applied in a variety of scientific disciplines [3–12]. In fact, chaos has been controlled successfully in various physical experiments, including a magnetic ribbon [6], a fluid convection system [7], a spin-wave system [8], a chemical system [9], an electric diode [10], laser systems [11], and cardiac systems [12]. Extension of the original method to control high-dimensional dynamical systems [4] and to control transient chaos [5] has also been investigated.

In this paper, we address the issue of controlling chaos in Hamiltonian systems. Our goal is to stabilize a chaotic orbit around some desired unstable periodic orbit for two-dimensional Hamiltonian maps. These maps may arise from surfaces of a section of two-degree-of-freedom time-independent Hamiltonian systems or from an experimental time series coming from a conservative process. At the first glance, one might think that the stabilization problem here is analogous to that in dissipative systems and, hence, the original OGY algorithm would apply to Hamiltonian systems in a straightforward way. That is not so, and the reason is that in Hamiltonian maps, due to area conservation, the Jacobian matrices evaluated along an unstable periodic orbit often exhibit complex-conjugate eigenvalues on the unit circle at some of its orbit points. This can be illustrated by using the much-studied standard map [13],

$$(x_{n+1},y_{n+1}) = [(x_n+y_n)\bmod(2\pi)-\pi, y_n+p\sin(x_n+y_n)] , \quad (1)$$

where p is the control parameter. Figure 1(a) shows a plot of the phase space for $p=1$, where the chaotic invariant set results from a single long trajectory. Most of the blank regions correspond to Kolmogorov-Arnold-Moser (KAM) islands and smaller chaotic invariant sets. Figures 1(b) and 1(c) show an unstable period-7 orbit and an unstable period-10 orbit, respectively, where the centers of the plus signs indicate the locations of the orbit points. The horizontal and vertical directions at each point signify the real and imaginary axes in the complex plane spanned by the eigenvalues. The nature of the pair of eigenvalues at each orbit point is schematically represented by two dots near the point (see figure captions). We see that it is quite common for an orbit point to possess complex-conjugate eigenvalues. We have also examined a large number of other periodic orbits and found similar mixing of real and complex-conjugate

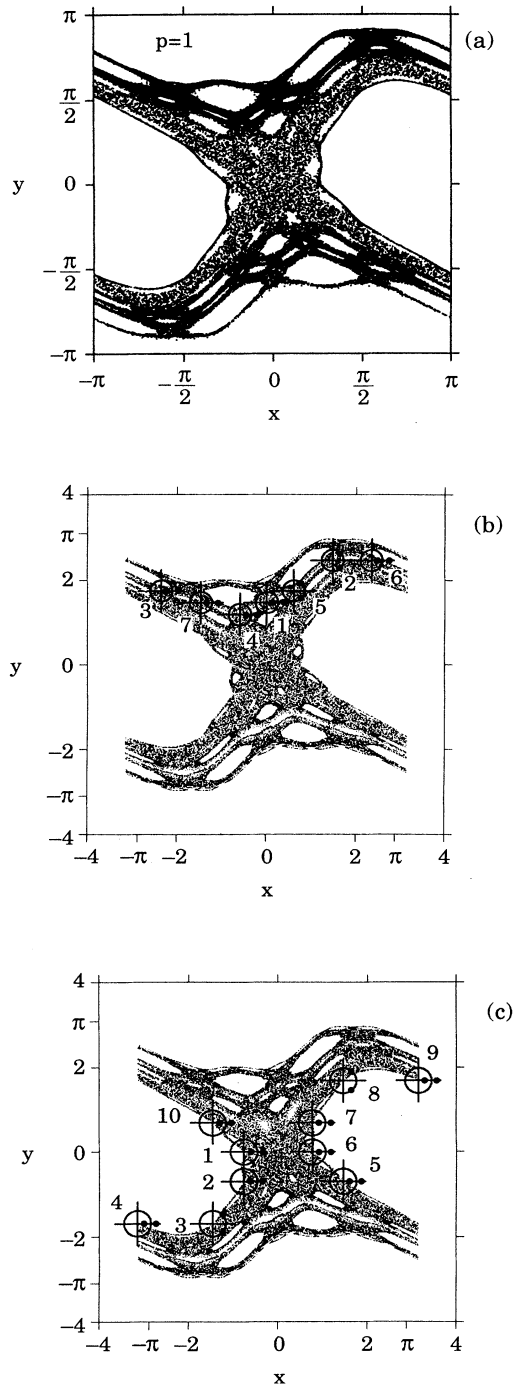

FIG. 1. (a) A single chaotic trajectory in the standard map [Eq. (1) with $p=1$] originated from the initial condition $(x_0,y_0)=(0.5,0.5)$. Notice the sharp contrast of the particle density in different phase-space regions. This is a manifestation of the "layered" structure of Hamiltonian systems. (b) and (c) The locations of a period-7 orbit and a period-10 orbit in the chaotic region, respectively. Eigenvalues associated with each orbit point are schematically represented by two dots. If the two dots are on the horizontal axis the periodic point has real eigenvalues, and if the two dots are on the circle then the point possesses complex-conjugate eigenvalues. The integers denote the order of orbit points under iterations of the map.

eignvalues along these orbits. In fact, one can show analytically (by studying the Jacobian matrix) that this is a general feature of the standard map when it is far from hyperbolicity.

Due to the existence of complex-conjugate eigenvalues on the unit circle along an unstable orbit, the original OGY formula for calculating the temporal-parameter perturbation generally fails to apply in Hamiltonian systems because it is expressed in terms of the real eigenvalues and eigenvectors along the periodic orbit [1] (see below for details). One might argue that since the periodic orbit itself is unstable, parameter perturbations can still be applied at every mth time step if the period of the desired orbit is m. In this way, the original OGY formula again becomes applicable. Although this is a viable approach for noise-free Hamiltonian systems, it is extremely vulnerable to external or system noises, particularly if the period of the desired orbit is large [14]. Hence, it is desirable to use an extension of the OGY method to allow for parameter perturbations at *each* time step of the system.

Our work starts by generalizing the original OGY formula to a form in which the temporal-parameter perturbations are expressed both in terms of the Jacobian matrix and of the unstable direction along a periodic orbit. Such a form is useful because although individual points along a periodic orbit can have complex-conjugate eigenvalues (and hence the eigenvectors are not defined in the real plane), these points still necessarily possess stable (contracting) and unstable (expanding) directions. To see how this arises we consider a small circle at one of the periodic-orbit points, say $\mathbf{X}_n$. By iterating the circle backward one step, we typically arrive at an ellipse around $\mathbf{X}_{n-1}$. Similarly, the image of a circle at $\mathbf{X}_{n-1}$ under $\mathbf{F}$ is generally an ellipse at $\mathbf{X}_n$. This indicates that there is a direction in the neighborhood of $\mathbf{X}_{n-1}$ along which the distance contracts and another direction along which the distance expands. The images of these two directions approximate the stable and unstable directions at $\mathbf{X}_n$. Thus the key point is to utilize these two directions in place of the stable and unstable eigenvectors in the original OGY formula [1]. (Later in this paper we will discuss an algorithm developed for a different problem [15] to calculate the stable and unstable directions at a given point.) The resulting formalism enables us to apply control at each time step during the evolution of the system. We will demonstrate the effectiveness of this approach by numerical examples.

Another issue arising in controlling Hamiltonian chaos concerns the length of the initial chaotic transient τ before a trajectory can be stabilized. The length of such a chaotic transient depends sensitively on the initial condition. In dissipative chaotic systems, for randomly chosen initial conditions, τ has an exponential probability distribution [16], i.e., $P(\tau)\sim\exp[-(\tau/\langle\tau\rangle)]$ for large τ, where $\langle\tau\rangle$ is the average length of time for control, and it scales with the maximum-allowable parameter perturbation as a power law [1]. Hence, in this case, $\langle\tau\rangle$ is always finite. In Hamiltonian systems, however, the probability distribution of τ is algebraic [17]: $P(\tau)\sim\tau^{-\alpha}$ for large τ, where α is the decay exponent with a value between 1 and 2. Hence, in this case, the average length of time for

control $\langle\tau\rangle$ is infinite. In practice, such a long time for control poses a major difficulty in controlling Hamiltonian chaos. It is thus necessary to "guide" a given initial condition to the desired controlling region (the neighborhood of the periodic orbit) in an efficient way before being able to stabilize the periodic orbit. Such a "targeting" algorithm has been proposed for dissipative systems [21] and it can be applied directly to some cases we consider in this paper [22]. However, since the main purpose of the present paper is on the application of the OGY method to Hamiltonian systems, we will only briefly discuss special features of targeting in Hamiltonian systems.

The organization of the paper is as follows. In Sec. II we review the basic theory of the OGY method and derive an expression for temporal-parameter perturbations that does not explicitly involve the eigenvalues. In Sec. III, we describe a method to calculate the stable and unstable directions along a trajectory (which can be either periodic or chaotic). In Sec. IV, we present our numerical results for the standard map and briefly discuss the issue of targeting and the effect of external noise. In Sec. V, we present the conclusion.

II. THE CONTROL METHOD

We consider the following discrete time dynamical system,

$$\mathbf{X}_{i+1}=\mathbf{F}(\mathbf{X}_i,p) , \tag{2}$$

where $\mathbf{X}_i\in\mathbb{R}^2$, $p\in\mathbb{R}$ is an externally controllable parameter, and $\mathbf{F}$ is a smooth function in both variables. Since we do not want to change the dynamics substantially, we restrict our parameter perturbation to be small. In other words, we require

$$|p-p_0|<\delta , \tag{3}$$

where p_0 is some nominal parameter value and δ is a small number defining the range of parameter variation. Our objective is to program the parameter p in such a way that a typical trajectory in the chaotic region is stabilized around some desirable unstable periodic orbit after an initial chaotic transient. The procedure is as follows. First we choose the periodic orbit that yields the best system performance. Next, we define a small region around each of the periodic-orbit points whose size is proportional to δ. Suppose the particle starts with some initial condition in the chaotic region. Due to the ergodicity, there is a certain probability that the particle will enter the small region around one of the periodic-orbit points. In a typical Hamiltonian system, due to the "stickiness" effect [18–20] of the KAM islands, the initial transient could be very long (to be discussed below). Once the particle is inside the small region, p will be judiciously changed to keep the trajectory around the periodic orbit.

Specifically, assume that the unstable orbit of period m to be controlled is

$$\mathbf{X}_{O1}(p)\rightarrow\mathbf{X}_{O2}(p)\rightarrow\cdots\rightarrow\mathbf{X}_{Om}(p)\rightarrow\mathbf{X}_{O(m+1)}(p)=\mathbf{X}_{O1}(p) .$$

The linearized dynamics in the neighborhood of the period-m orbit is

$$\mathbf{X}_{n+1}-\mathbf{X}_{O(n+1)}(p_n)=\mathbf{M}\cdot[\mathbf{X}_n-\mathbf{X}_{On}(p_n)] , \tag{4}$$

where $\mathbf{M}$ is the two-dimensional Jacobian matrix at the orbit point $\mathbf{X}_{On}$, $p_n=p_0+(\Delta p)_n$, $(\Delta p)_n\le\delta$. Note that the parameter variation will result in the following shift of the periodic-orbit points:

$$\mathbf{X}_{On}(p_n)-\mathbf{X}_{On}(p_0)\approx(\Delta p)_n\mathbf{g}_n , \tag{5}$$

where $\mathbf{g}_n=\partial\mathbf{X}_{On}(p)/\partial p|_{p_0}$.

In Eq. (4), we will not express the Jacobian matrix $\mathbf{M}$ in terms of eigenvalues and eigenvectors because there may exist complex-conjugate eigenvalues on the unit circle at some of the periodic points. Instead we explore the stable and unstable directions associated with these points. The stable and unstable directions do not necessarily coincide with the eigenvectors [15] at a given periodic point if $m\neq1$. In the case of complex-conjugate eigenvalues, those eigenvectors are not even defined in the real plane. The existence of both stable and unstable directions around each orbit point can be seen as follows. Let us choose a small circle of radius ϵ at some orbit point $\mathbf{X}_{On}$. In a Cartesian coordinate system with the origin at $\mathbf{X}_{On}$, the circle can be expressed as $dx^2+dy^2=\epsilon^2$. The image of the circle under $\mathbf{F}^{-1}$ in the Cartesian coordinate system with the origin at $\mathbf{X}_{O(n-1)}$ can be expressed as $A(dx')^2+B(dx')(dy')+C(dy')^2=1$, which is typically an ellipse. Here A, B, and C are functions of the entries of the inverse Jacobian matrix at $\mathbf{X}_{On}$. This deformation from a circle to an ellipse means that the distance along the major axis of the ellipse at $\mathbf{X}_{O(n-1)}$ contracts as a result of the map. Similarly, the image of a circle at $\mathbf{X}_{O(n-1)}$ under $\mathbf{F}$ is typically an ellipse at $\mathbf{X}_{On}$. This means that the distance along the inverse image of the major axis of the ellipse at $\mathbf{X}_{On}$ expands under $\mathbf{F}$. Thus the major axis of the ellipse at $\mathbf{X}_{O(n-1)}$ and the inverse image of the major axis of the ellipse at $\mathbf{X}_{On}$ approximate the stable and unstable directions at $\mathbf{X}_{O(n-1)}$. In Sec. III, we discuss a systematic method of finding these stable and unstable directions for general two-dimensional maps.

Let $\mathbf{e}_{s(n)}$ and $\mathbf{e}_{u(n)}$ be the stable and unstable directions at $\mathbf{X}_{On}$, and let $\mathbf{f}_{s(n)}$ and $\mathbf{f}_{u(n)}$ be two vectors that satisfy $\mathbf{f}_{u(n)}\cdot\mathbf{e}_{u(n)}=\mathbf{f}_{s(n)}\cdot\mathbf{e}_{s(n)}=1$ and $\mathbf{f}_{u(n)}\cdot\mathbf{e}_{s(n)}=\mathbf{f}_{s(n)}\cdot\mathbf{e}_{u(n)}=0$. To control the orbit, we require that the next iteration of a trajectory point after falling into one of the small neighborhoods around $\mathbf{X}_{On}$ lies on the stable direction at $\mathbf{X}_{O(n+1)}(p_0)$, i.e.,

$$[\mathbf{X}_{n+1}-\mathbf{X}_{O(n+1)}(p_0)]\cdot\mathbf{f}_{u(n+1)}=0 . \tag{6}$$

Substituting Eqs. (4) and (5) into Eq. (6), we obtain the following expression for the parameter perturbations:

$$(\Delta p)_n=\frac{\{\mathbf{M}\cdot[\mathbf{X}_{n+1}-\mathbf{X}_{On}(p_0)]\}\cdot\mathbf{f}_{u(n+1)}}{[(\mathbf{M}\cdot\mathbf{g}_n)-\mathbf{g}_{n+1}]\cdot\mathbf{f}_{u(n+1)}} , \tag{7}$$

where $\mathbf{M}$ is evaluated at $\mathbf{X}_{On}(p_0)$. Note that the quantities in Eq. (7) are all experimentally accessible through the time-delay embedding method, although a slight

modification of Eq. (7) is required in such cases [2]. In particular, the Jacobian matrices and their inverses along a periodic orbit can be obtained by using the algorithm proposed by Eckmann and Ruelle [23]. We emphasize that the parameter perturbations calculated from Eq. (7) apply to the system at *each* time step, thus minimizing the effect of external noise [1,14]. It should also be noted that there are other ways to stabilize unstable periodic orbits, e.g., the "pole placement method" [4]. However, we believe [4] that parameter perturbations based on stable and unstable directions [Eq. (7)] are optimal.

III. CALCULATING STABLE AND UNSTABLE DIRECTIONS

Once we know the Jacobian matrices, the stable and unstable directions at each orbit point can be calculated, and $\mathbf{f}_{u(n+1)}$ in Eq. (7) can then be obtained. To achieve this, we use an algorithm developed in Ref. [15]. This algorithm can be applied to cases where the period of the orbit is arbitrarily large.

To find the stable direction at a point $\mathbf{X}$, we first iterate this point forward N times under the map $\mathbf{F}$ and get a trajectory $\mathbf{F}^1(\mathbf{X})$, $\mathbf{F}^2(\mathbf{X})$, ..., $\mathbf{F}^N(\mathbf{X})$, as schematically shown in Fig. 2(a). Now imagine we put a circle of arbitrarily small radius ϵ at the point $\mathbf{F}^N(\mathbf{X})$. If we iterate this circle backward once, the circle will become an ellipse at the point $\mathbf{F}^{N-1}(\mathbf{X})$ with the major axis along the stable direction of the point $\mathbf{F}^{N-1}(\mathbf{X})$. We continue iterating this ellipse backward, while at the same time keeping the ellipse's major axis of order ϵ via certain normalization procedures. When we iterate the ellipse all the way back to the point $\mathbf{X}$, the ellipse becomes very thin, with its major axis along the stable direction at point $\mathbf{X}$ provided N is large enough.

In practice, instead of using a small circle, we take a unit vector at the point $\mathbf{F}^N(\mathbf{X})$, since the Jacobian matrices of the *inverse map* $\mathbf{F}^{-1}$ rotates a vector in the tangent space of $\mathbf{F}$ towards the stable direction. Thus we iterate a unit vector backward to the point $\mathbf{X}$ by multiplying by the Jacobian matrices of the inverse map at each point on the *already existing* orbit. A key point in the calculation is that we do *not* actually calculate the inverse Jacobian matrix along the trajectory *by* iterating the point $\mathbf{F}^N(\mathbf{X})$ backwards using the inverse map $\mathbf{F}^{-1}$. The reason is that if we do so, the trajectory will usually diverge from the original trajectory $\mathbf{F}^N(\mathbf{X})$, $\mathbf{F}^{N-1}(\mathbf{X})$, ..., $\mathbf{F}^1(\mathbf{X})$ after only a few backward interactions. What we do is to store the inverse Jacobian matrix at every point of the orbit $\mathbf{F}^i(\mathbf{X})$ $(i=1,\ldots,N)$ when we iterate forward the point $\mathbf{X}$ beforehand. We normalize the vector after each multiplication to the unit length. For sufficiently large N, the unit vector we get at $\mathbf{X}$ is a good approximation of the stable direction at $\mathbf{X}$.

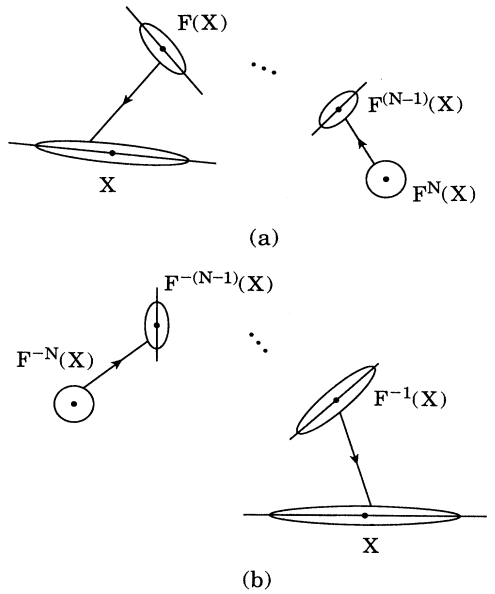

FIG. 2. A schematic illustration of our method to find (a) the stable and (b) the unstable directions for a trajectory point $\mathbf{X}$.

Similarly, as shown schematically in Fig. 2(b), to find the unstable direction at point $\mathbf{X}$, we first iterate $\mathbf{X}$ backward under the inverse map N times to get a backward orbit $\mathbf{F}^{-j}(\mathbf{X})$ $(j=N,\ldots,1)$. We then choose a unit vector at point $\mathbf{F}^{-N}(\mathbf{X})$ and iterate this unit vector forward to point $\mathbf{X}$ along the already existing orbit by multiplying by the Jacobian matrix of the map N times since the Jacobian matrix of the forward map rotates a vector towards the unstable direction. We normalize the vector to the unit length at each step. The final vector at point $\mathbf{X}$ is a good approximation of the unstable direction at that point if N is large enough. Again, to avoid divergence from the original trajectory, we do not actually iterate the inverse map. What we do in this case is to choose $\mathbf{X}$ to be the end point of a forward orbit, all the points before $\mathbf{X}$ are the inverse images of $\mathbf{X}$, and we store the Jacobian matrices of the forward map at those points.

The method so described is very efficient. Particularly, it converges fast. For $N=20$, the error between the calculated and real stable (or unstable) directions is on the order of 10^{-10} for chaotic trajectories in the Hénon map [15]. For the standard map we find a similar rate of convergence.

IV. NUMERICAL RESULTS AND DISCUSSIONS

We have successfully controlled all the unstable periodic orbits we set out to control for the standard map of Eq. (1) by perturbing the parameter p. Figure 3(a) shows the result of stabilizing the period-7 orbit in Fig. 1(b). Here the horizontal axis is time and the vertical axis is the x projection of the orbit. Figures 3(b) and 3(c) show the result for controlling the period-10 orbit in Fig. 1(c). In both cases, we start a chaotic trajectory from the initial condition $(x_0,y_0)=(0.02,0.02)$. As soon as the trajectory falls into a small circle of radius 0.01 around any one of the periodic-orbit points, the temporal-parameter control of Eq. (7) is turned on to stabilize the trajectory around the periodic orbits. We set $\delta=0.01$ in both cases. An interesting feature of the time series in Figs. 3(a)–3(c) is the appearance of "holes" in the uncontrolled trajectory. These holes are the consequence of the stickiness effect of KAM islands. Namely, when the trajectory enters the neighborhood of some KAM islands associated with an elliptic periodic orbit, they tend to stay near the islands

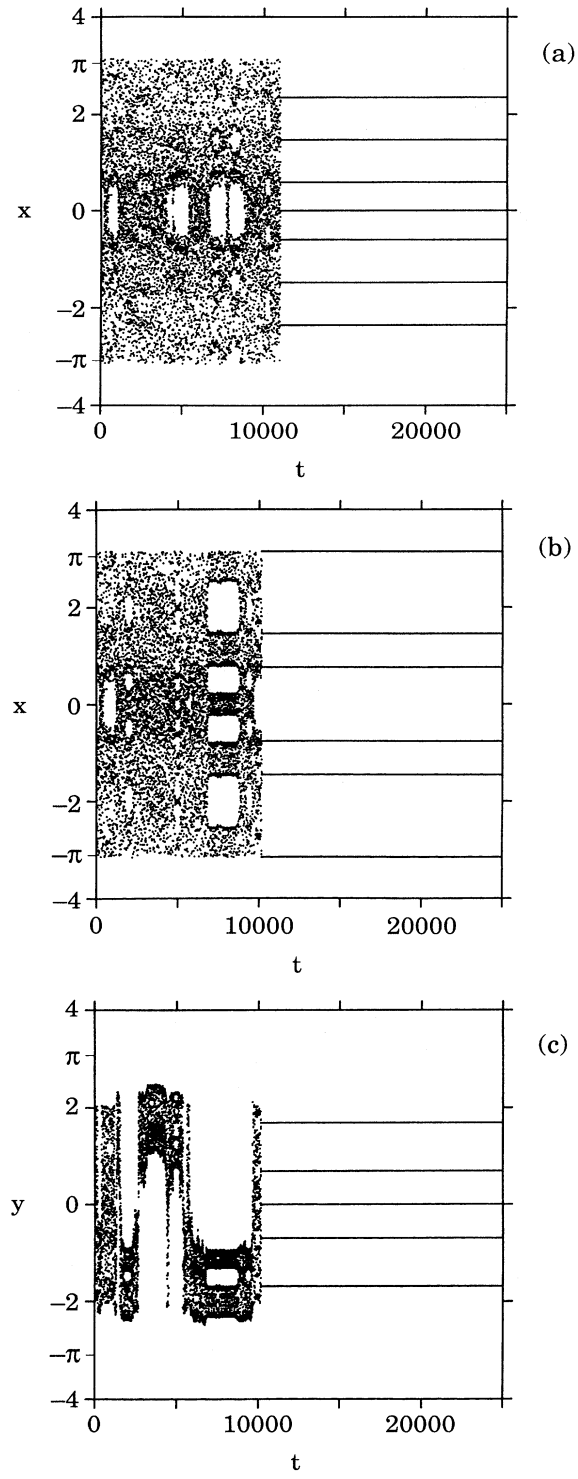

FIG. 3. Time series for stabilizing (a) the period-7 orbit [corresponding to Fig. 1(b)] (x projection). (b) and (c) x and y projections, respectively, of stabilizing the period-10 orbit [corresponding to Fig. 1(c)]. In (a)–(c), the initial condition is $(x_0,y_0)=(0.02,0.02)$ and $\delta=0.01$. Note that the initial chaotic transient is on the order of 10^4. In (b), only six distinct values of x are seen. The reason is because four pairs of the period-10 orbit have the same x values. A similar explanation applies to (c), where only five distinct y values are seen.

for a long time. When this occurs, the trajectory wanders around the KAM islands and spares the chaotic region in between the KAM islands, thus leaving unfilled regions in the projection of the trajectory on the x or y axis.

Another feature in Figs. 3(a)–3(c) is that the initial chaotic transient before the trajectory can be stabilized is quite long (on the order of 10^4 in these cases). This is again due to the stickiness effect of KAM islands. In dissipative chaotic systems the average length of time for control $\langle\tau\rangle$ scales with the predefined range δ of parameter perturbations [cf. Eq. (3)] as [1]

$$\langle\tau\rangle\sim\delta^{-\gamma}\,, \tag{8}$$

where γ (finite) is a scaling exponent. So in this case, $\langle\tau\rangle$ is finite if $\delta\neq 0$. In contrast, in Hamiltonian systems, $\langle\tau\rangle$

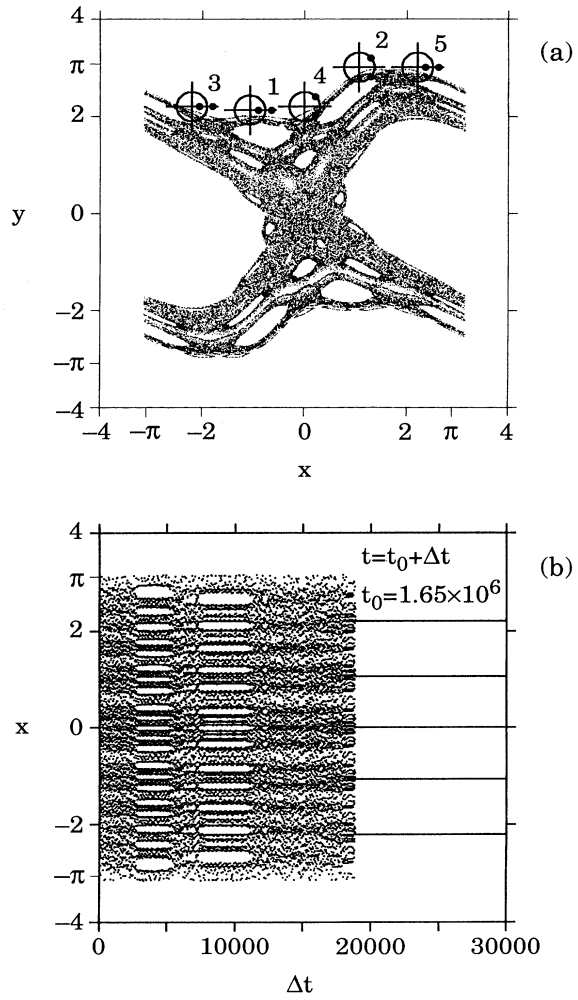

FIG. 4. An example of an extremely long chaotic transient (on the order of 10^6) that arises in the case of stabilizing a period-5 orbit. (a) The locations and eigenvalues of the period-5 orbit. (b) Time series of x before and after the stabilization. Initial condition of the trajectory is $(x_0,y_0)=(0.5,0.5)$ and $\delta=0.01$. This superlong chaotic transient arises because the period-5 orbit and the initial condition are apparently in different "layers" of the phase space separated by Cantori (remains of KAM surfaces) [see Fig. 1(a) and text].

can be expresed as

$$\langle \tau \rangle \sim \int \tau^{1-\alpha} d\tau \,, \tag{9}$$

which diverges for typical values of the decay exponent α ($\alpha \approx 1.45$ in Karney's numerical experiment [18], $\alpha \approx 1.34$ in Chirikov and Shepelyansky's numerical experiment [19], and $\alpha < 1.96$ in a theory based on a Markov-tree model by Meiss and Ott [20]). In practice, this means that the average transient could be extremely long regardless of the magnitude of δ. Figures 4(a) and 4(b) show such a case in which the periodic orbit to be controlled is a period-5 orbit. Figure 4(a) shows the locations and the nature of eigenvalues of the orbit and Fig. 4(b) shows the chaotic transient and the stabilized orbit. Note that the beginning time in Fig. 4(b) has been reset to 0 after an initial time of 1.65×10^6. In other words, the transient in this case is on the order of 10^6. This situation of an extremely long chaotic transient in controlling Hamiltonian chaos (in the presence of KAM surfaces) is fundamentally different from the situation of controlling dissipative chaotic attractors.

A possible solution to the problem of long chaotic transients is "targeting" [21], in which a point is brought rapidly to the desired place ("target") in the phase space via small parameter perturbations. However, in Hamiltonian systems, the phase space is divided into layered components which are separated from each other by Cantori [24], remains of KAM surfaces. One typically observes that particles initialized in one layer of the chaotic region wander in that layer for a long period of time before they cross the Cantori and wander in the next layer. This fact can also be seen in Fig. 1(a), where the density of particles in different layers shows sharp contrast. If an initial condition and the intended target are in the same layer, the conventional targeting method [21] is expected to apply directly [22]. When the initial condition and the target are in different layers, however, it is not clear whether such a targeting method can *effectively* bring the particle from one layer to another and then to the target. Thus devising a general scheme of targeting for the layered Hamiltonian phase-space structure is still an open question.

Finally, we briefly discuss the influence of external noise in controlling Hamiltonian chaos. In the presence of noise (say, with a Gaussian probability distribution), a trajectory stabilized around an unstable periodic orbit will occassionally be "kicked" out of the neighborhood of that periodic orbit [1]. To effectively achieve the control, the magnitude of the parameter perturbation must exceed the average amplitude of the noise. Even so, there is still a probability of the controlled trajectory being kicked out. In dissipative systems, this may not be as serious a problem because after a relatively short chaotic transient, the trajectory will move back to the desired controlling region. In Hamiltonian systems, however, when this occurs, the trajectory may experience an extremely long transient before it comes close to the controlling region, as mentioned above. It is then necessary to apply the targeting method to bring the trajectory back after it is kicked out by the noise. Consequently, we believe that an efficient and practically applicable package of controlling Hamiltonian chaos would contain both the control algorithm developed in this paper and a targeting algorithm yet to be developed.

V. CONCLUSION

The major contribution of the present work is an extension of the original OGY stabilization method of controlling dissipative chaos to chaotic Hamiltonian systems, where unstable periodic orbits often possess complex-conjugate eigenvalues on the unit circle [25]. Particularly, we have used an expression for the temporal-parameter perturbations not explicitly involving the eigenvalues and eigenvectors at each periodic-orbit point. This is done by utilizing the stable and unstable directions associated with each orbit point. In addition, we have presented an efficient algorithm to calculate the stable and unstable directions for a periodic orbit. We have also discussed the effect of KAM islands on the control, which leads us to believe that a targeting algorithm will be an important ingredient in achieving a practical control of Hamiltonian chaos.

ACKNOWLEDGMENTS

We thank Tamàs Tél for valuable comments. This work was supported by the U.S. Department of Energy (Scientific Computing Staff, Office of Energy Research).

[1] E. Ott, C. Grebogi, and J. A. Yorke, Phys. Rev. Lett. **64**, 1196 (1990); in *Chaos: Soviet-American Perspectives on Nonlinear Science,* edited by D. K. Campbell (American Institute of Physics, New York, 1990).
[2] U. Dressler and G. Nitsche, Phys. Rev. Lett. **68**, 1 (1992).
[3] D. Auerbach, C. Grebogi, E. Ott, and J. A. Yorke (unpublished).
[4] F. J. Romeiras, C. Grebogi, E. Ott, and W. P. Dayawansa, Physica D **58**, 165 (1992).
[5] T. Tel, J. Phys. A **24**, L1359 (1991).
[6] W. L. Ditto, S. N. Rauseo, and M. L. Spano, Phys. Rev. Lett. **65**, 3211 (1990).
[7] J. Singer, Y.-Z. Wang, and H. H. Bau, Phys. Rev. Lett. **66**, 1123 (1991).
[8] A. Azevedo and S. M. Rezende, Phys. Rev. Lett. **66**, 1342 (1991).
[9] B. Peng, V. Petrov, and K. Showalter, J. Phys. Chem. **95**, 4957 (1991).
[10] E. R. Hunt, Phys. Rev. Lett. **67**, 1953 (1992).
[11] R. Roy, T. W. Murphy, Jr., T. D. Maier, and Z. Gills, Phys. Rev. Lett. **68**, 1259 (1992); C. Reyl, L. Flepp, R. Badii, and E. Brun (unpublished).
[12] A. Garfinkel, W. L. Ditto, M. L. Spano, and J. Weiss, Science **257**, 1230 (1992).
[13] B. V. Chirikov, Phys. Rep. **52**, 263 (1979).
[14] Note that a trajectory originally in the neighborhood of

a period-m orbit leaves the orbit exponentially like $\exp(\lambda_u m)$, where $\exp(\lambda_u)>1$ is the unstable Lyapunov number of the orbit. Under the influence of noise, if control is applied at every mth time step, the trajectory will deviate from the orbit rapidly before the next parameter control can be applied and one may lose control. Hence, it is desirable that the control be applied at *each* time step.

[15] Y. C. Lai, C. Grebogi, J. A. Yorke, and I. Kan, Nonlinearity (to be published).

[16] C. Grebogi, E. Ott, and J. A. Yorke, Phys. Rev. Lett. **57**, 1284 (1986); P. Romeiras, C. Grebogi, E. Ott, and J. A. Yorke, Phys. Rev. A **36**, 5365 (1987).

[17] The algebraic probability distribution of τ in Hamiltonian systems can be seen as follows. The phase space of typical Hamiltonian systems consists of KAM islands and chaotic regions. The KAM islands appear to exist in all scales and typically form an island-around-island phase-space structure. Hence, a particle initialized in the chaotic region may spend an arbitrarily long time in the island-around-island structure. A physical consequence of this is that particles exit algebraically [18–20] from some predefined (large) phase-space region containing the island-around-island structure. To be specific, imagine that there is some large region surrounded by an outermost KAM island curve and that outside this island there is a connected chaotic region. We then draw a large circle which contains the large island at its center and which also encloses a substantial part of the outer chaotic region. Now initialize a large number of randomly chosen initial conditions in the connected chaotic region outside the large island and evolve them under the dynamics. If a particle leaves the circle, we regard it as having exited the system. Let $P(t)$ denote the probability of particles inside the circle at time t; then one typically observes [18] that $P(t)\sim t^{-\alpha}$.

[18] C. F. F. Karney, Physica D **8**, 360 (1983).

[19] B. V. Chirikov and D. L. Shepelyansky, Physica D **13**, 395 (1984).

[20] J. D. Meiss and E. Ott, Phys. Rev. Lett. **55**, 2741 (1985); Physica D **20**, 387 (1986).

[21] T. Shinbrot, E. Ott, C. Grebogi, and J. A. Yorke, Phys. Rev. Lett. **65**, 3215 (1990).

[22] T. Shinbrot (private communication).

[23] J.-P. Eckmann and D. Ruelle, Rev. Mod. Phys. **57**, 617 (1985).

[24] R. S. Mackay, J. D. Meiss, and I. C. Pervival, Phys. Rev. Lett. **52**, 697 (1984); and Physica D **13**, 55 (1984).

[25] After we completed the present work, we received a report by C. Reyl, L. Flepp, R. Badii, and E. Brun, who demonstrated the control of NMR-laser chaos in high-dimensional embedding space. In their system, there also exist complex eigenvalues. Since the system is dissipative, those complex eigenvalues are not on the unit circle. They developed a modified OGY method in which parameter perturbations are chosen to minimize the norm $\|\mathbf{X}_{n+1}-\mathbf{X}_{O(n+1)}(p_0)\|$ contained in Eq. (4). Hence, their method does not make use of the geometric structure of hyperbolic period orbits, and consequently is quite different from the method we present in this paper.